Climatic Change (2023) 176:142
https://doi.org/10.1007/s10584-023-03606-0

Ground-based climate data show evidence of warming and intensification of the seasonal rainfall cycle during the 1960–2020 period in Yangambi, central Congo Basin

Emmanuel Kasongo Yakusu[1,2,3] · Joris Van Acker[1] · Hans Van de Vyver[4] · Nils Bourland[2,5,6] · José Mbifo Ndiapo[7] · Théophile Besango Likwela[7] · Michel Lokonda Wa Kipifo[7] · Amand Mbuya Kankolongo[8] · Jan Van den Bulcke[1] · Hans Beeckman[2] · Marijn Bauters[9,10] · Pascal Boeckx[9] · Hans Verbeeck[10] · Kim Jacobsen[2,10] · Gaston Demarée[4] · Françoise Gellens-Meulenberghs[4] · Wannes Hubau[1,2]

Received: 22 August 2022 / Accepted: 7 September 2023 / Published online: 5 October 2023
© The Author(s) 2023

Abstract
Meteorological stations are rare in central Africa, which leads to uncertainty in regional climatic trends. This is particularly problematic for the Congo Basin, where station coverage decreased significantly during the last few decades. Here, we present a digitized dataset of daily temperature and precipitation from the Yangambi biosphere reserve, covering the period 1960–2020 (61 years) and located in the heart of the Congo Basin. Our results confirm a long-term increase in temperature and temperature extremes since the 1960s, with strong upward trends since the early 1990s. Our results also indicate a drying trend for the dry season and intensification of the wet season since the early 2000s. Ongoing warming and increasing precipitation seasonality and intensity already have a significant impact on crop yields in Yangambi. This calls for urgent development of climate-smart and dynamic agriculture and agroforestry systems. We conclude that systematic digitization and climate recording in the Congo Basin will be critical to improve much-needed gridded benchmark datasets of climatic variables.

Keywords Congo Basin · Warming · Precipitation seasonality · Digitization · Historical data · Station coverage

1 Introduction

Several authors report evidence of a drying trend in central Africa during the last few decades, based on available interpolated gridded climate datasets (Tsalefac et al. 2015; Dezfuli and Dezfuli 2017; Nicholson et al. 2018b, 2019; Mabrouk et al. 2022) and satellite products (Diem et al. 2014; Zhou et al. 2014). This drying trend started between 1990 and 2000 and is thought to be one of the most significant worldwide (Malhi and Wright 2004;

Extended author information available on the last page of the article

Asefi-Najafabady and Saatchi 2013; Zhou et al. 2014; Nicholson et al. 2018b). The long-term drying trend in central Africa was recently supported by in-depth analysis of multiple independent precipitation and satellite-derived vegetation datasets, showing that the dry season length increased by 6.4–10.4 days per decade in the period 1988–2013, due to an earlier dry season onset and a delayed dry season end (Jiang et al. 2019). Furthermore, some climate model projections show decreasing precipitation towards the end of the twenty-first century under several RCP scenarios (Fotso-Nguemo et al. 2017). At the same time, wet and dry extreme events are expected to become more frequent and more severe (Fotso-Nguemo et al. 2018; Kendon et al. 2019; Karam et al. 2022).

Nevertheless, large uncertainties on past and future central African climate variability persist because meteorological stations are rare in central Africa (Aguilar et al. 2009; Chaney et al. 2014; Kidd et al. 2017; Nicholson et al. 2018a; Bush et al. 2020; Nicholson 2022). While central Africa was covered by up to 1000 climate stations in the 1960s, 1970s, and 1980s, the network dramatically collapsed afterwards (Nicholson et al. 2018b; Nicholson 2022) (Fig. 1). Especially, the Democratic Republic of the Congo has been poorly covered in recent decades, with only 17 climate stations providing data for the 2000–2016 period. All these stations are located in the South-West of the country, leaving a large gap of more than a million km^2 in the central rainforest area (Fig. 1). This data gap exists due to long-lasting political instabilities and restricted data-sharing policies, which impeded data acquisition, data digitization, and use of the data in a scientific context (Dezfuli and Dezfuli 2017; Nicholson et al. 2018b). Furthermore, satellite products often do not perform well in the tropics (McCollum et al. 2000; Awange et al. 2016; Sun et al. 2018; Nicholson et al. 2019; Igri et al. 2022). This leads to substantial uncertainty in regional long-term climate trends (Washington et al. 2013; Awange et al. 2016). Uncertainties are especially high for rainfall due to high spatial variability in precipitation regimes (Kidd et al. 2017; Bush et al. 2020). Additional to these uncertainties, regional and global climate models show opposing future trends for most of central Africa, suggesting that both past and projected climate change signals may not be robust (Dosio et al. 2019).

Yet, a good understanding of climate variability is of utmost importance to predict potential impact of future climate change in central Africa. Continued long-term drying or intensification of extreme events may likely have large impact on tropical forest composition, functioning, and carbon sequestration (Fauset et al. 2012; Denbow 2013; Zhou et al. 2014; Aguirre-Gutiérrez et al. 2020; Hubau et al. 2020; Bennett et al. 2021). Furthermore, climate change has large impacts on forestry, agriculture, agroforestry and health (Verchot et al. 2007; Diem et al. 2014; Salerno et al. 2019; Tschora and Cherubini 2020). Hence, it is of utmost importance to further investigate central African climate trends by collecting much-needed ground-based data. To do so, the Trans-African Hydro-Meteorological Observatory (TAHMO) is developing a network of modern weather stations across central Africa, which is monitoring climate since 2015 and will continue to do so in the future. Yet, long-term records including historical data are equally important to analyze long-term climate variability and to compare with climate model simulations of past and projected future changes.

Therefore, we visited the climate station of the Yangambi Man-and-the-Biosphere reserve, which is a leading research site in the Democratic Republic of the Congo and is located in the heart of the data-poor area in central Africa (Fig. 1). Although the Yangambi data were not digitized since the 1990s, the station remained operational. We digitized the daily temperature and precipitation observations for the period covering 1960 to 2020 (61 years), we calculated monthly and yearly meteorological indices (describing temperature extremes, rainfall intensity, water demand and availability, drought and seasonality),

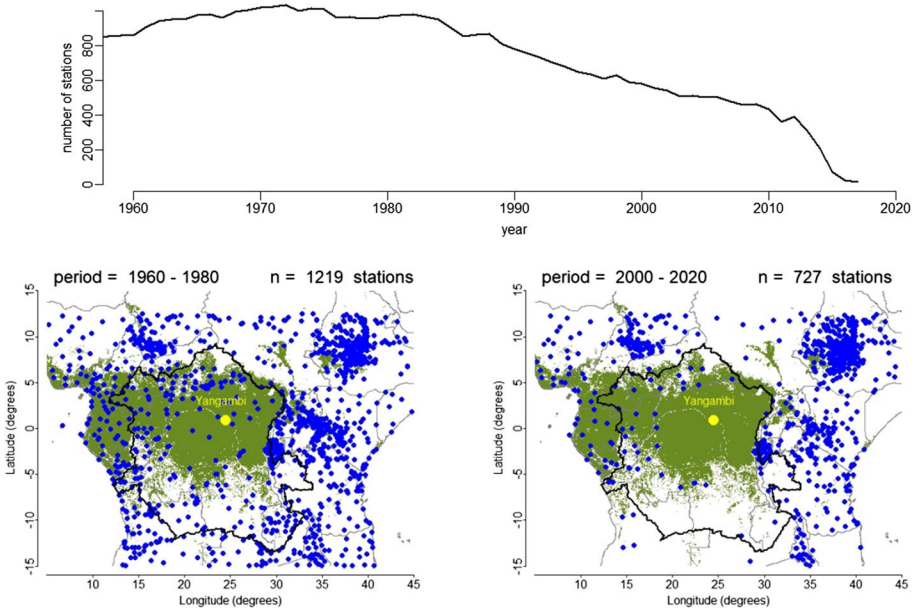

Fig. 1 Evolution and geographic position of climate stations with available precipitation data in and around the Congo Basin (outlined in thick black line). The top panel represents the evolution of the number of stations with digitized climate data for the last six decades (1960–2020) (Nicholson et al. 2018b). The two maps represent the geographic position of the stations with digitized climate data for two-decadal periods (1960–1980 and 2000–2020). Each blue dot in the maps represents a climate station; the yellow dot in the center of each map represents the Yangambi climate station (N 00° 49′ 12.4″; E 024° 27′ 22.6″). Green background color represents closed tropical rainforest cover following Global Landcover Map 2000 (Mayaux et al. 2003)

and we performed long-term and piecewise linear regression to detect long- or short-term trends. We used this analysis to address the following questions: (1) how did temperature and temperature extremes vary in Yangambi (Fig. 2); (2) how did precipitation and rainfall intensity vary in the dry and wet season (Fig. 3); (3) how did water demand and precipitation seasonality vary (Fig. 4)? Finally, we investigated how well observed records of precipitation and temperature from the Yangambi meteorological station compare with those from existing gridded datasets (Fig. 5 and Fig. 6)?

2 Data and methods

2.1 Yangambi station and daily meteorological measurements

The study was carried out in the UNESCO Biosphere Reserve of Yangambi. The reserve covers an area of 230,000 ha and is situated ~ 100 km west of Kisangani, at the banks of the Congo River and just north of the equator in the Tshopo Province (Democratic Republic of Congo), between 0° 49′–0° 51′N and 24° 29′–24° 35′E (Fig. 1). Vegetation in Yangambi consists mainly of moist semi-deciduous rainforest, with patches of moist evergreen

rainforest (in river valleys), transition forest, and agricultural land (Mangaza et al. 2021). Four forest types are found in Yangambi: (i) young secondary forest dominated by pioneer species such as *Musanga cecropioides* R. Br. ex Tedlie and *Macaranga monandra* Müll. Arg.; (ii) semi-deciduous mixed forest dominated by long-lived pioneer species such as *Pericopsis elata* (Harms) Meeuwen; (iii) semi-deciduous mixed forest dominated by shade-tolerant species such as *Scorodophloeus zenkeri* Harms; and (iv) evergreen monodominant forests dominated by *Gilbertiodendron dewevrei* (De Wild.) J. Léonard or *Brachystegia laurentii* (De Wild.) Louis ex Hoyle (Luambua et al. 2021). Yangambi has the Af climate according to the Köppen classification with a slightly marked dry season, an average annual precipitation of 1837 mm, and mean annual temperature of 25.1 °C.

The Yangambi meteorological station is managed by the INERA (*Institut National pour l'Étude et la Recherche Agronomiques*). It is positioned on a large plateau to avoid topographical influences. The site of the station is levelled, maintained regularly, and located far from the immediate influence of trees and buildings. The station records precipitation through an analog precipitation gauge (Casella London), which collects rainfall through a horizontal opening of known cross-section, and stores it in a test tube which is graduated (gauged) from 0 to 13 mm. Minimum (Tmin) and maximum (Tmax) temperature are recorded using two Hg thermometers placed inside a well-aerated housing in an open shelter. Meteorological data at Yangambi is recorded daily at 6 am, 9 am, 12, 15 pm, and 18 pm on paper sheets. Supplementary Fig. 1 shows an example of a manual record and pictures of the Yangambi climate station.

The precipitation gauges deployed at Yangambi have not been changed since their installation in 1928 and thermometers not since 1960. After digitization, data quality checks consisted of a visual inspection of the time series for the detection of possible typos, leading to unrealistic precipitation and extreme temperatures. These checks were complemented by direct comparisons with pictures of the original manual documents. As such, we digitized daily minimum temperature (in °C), daily maximum temperature (in °C), and daily precipitation (in mm), for the period between 1 January 1960 until 31 December 2020. There is a hiatus in the dataset from 1 December 1964 to 30 September 1965, when all activities at Yangambi were suspended due to political unrest. Hence, we excluded the year 1965 from our analysis. For December 1964, we estimated daily values of each variable by interpolating between the equivalent calendar days in 1963 and 1965.

To validate the analog measurements, a state-of-the-art meteorological station (Atmos 41, METER Group, Pullman, WA, USA) has been mounted next to the traditional Yangambi instrumentation in September 2018. This digital meteorological station is part of TAHMO, and data can be monitored in quasi real-time at https://tahmo.org/climate-data/. Digital recordings of daily minimum and maximum temperature as well as precipitation cover one full year of data, from 30 September 2018 until 30 September 2019 (365 days). Daily measurements of analog and digital devices are compared in Supplementary Fig. 2 and Supplementary Fig. 3, suggesting a consistent agreement between analog and digital data.

2.2 Monthly meteorological indices

To study climate variability, we considered monthly and yearly meteorological indices developed by the Expert Team on Climate Change Detection Monitoring Indices (ETCCDMI) from the World Climate Research Program of the World Meteorological

Organization (see Table 1 for index definitions). Indices were calculated on a monthly and/or annual basis using the daily meteorological measurements. All calculations were performed using the R statistical platform, version 3.2.1 (R Core Team 2017).

2.2.1 Temperature

We first calculated general temperature indices. These are the monthly average of the daily minimum temperature (ATN, in °C), the monthly average of the daily maximum temperature (ATX, in °C), the monthly average of the daily mean temperature (ATM, in °C), and the monthly average diurnal temperature range (DTR = ATX-ATN). Furthermore, we calculated monthly lowest (TXmin) and highest (TXmax) maximum daily temperature and monthly lowest (TNmin) and highest (TNmax) minimum daily temperature.

2.2.2 Rainfall

To quantify rainfall, we considered simple indices such as the monthly total precipitation (PTOT, in mm) and the monthly number of wet (or rainy) days (Rd, in days), with a wet day defined as a day with rainfall ≥ 1 mm. To quantify rainfall intensity, we calculated the monthly average rainfall from wet days, known as the simple day intensity index (SDII, in mm).

2.2.3 Standardized precipitation and evapotranspiration index

We then calculated the standardized precipitation evapotranspiration index (SPEI) at different time scales (3, 6, 12, 24, and 48 months). The SPEI index was developed by Vicente-Serrano et al. (2010). This index is the derivative of the SPI, a commonly used indicator to detect meteorological drought (precipitation deficits) (Mckee et al. 1993; Edwards and Mckee 1997). The fundamental difference between these two indicators is that SPI is calculated based on precipitation, while SPEI is based on the difference between precipitation and potential evapotranspiration (Karam et al. 2022) in including the role of temperature. The procedure to calculate the SPEI index involves a climatic water balance, the accumulation of deficit/surplus at different time scales, and adjustment to a log-logistic probability distribution (Vicente-Serrano et al. 2010). For each decade within our record, we calculated the drought duration as the number of months in drought conditions according to the different SPEI values.

2.3 Yearly meteorological indices

Apart from monthly meteorological indices, we also calculated and analyzed yearly indices to fully explore the data. Monthly and yearly indices allow using different statistical approaches to test long-term trends.

2.3.1 Temperature

General temperature indices are the annual average of the daily minimum temperature (ATN, in °C), the annual average of the daily maximum temperature (ATX, in °C), the annual average of the daily mean temperature (ATM, in °C), and the annual average diurnal temperature range (DTR). Furthermore, we calculated annual lowest (TXmin) and highest (TXmax) maximum daily temperature and annual lowest (TNmin) and highest (TNmax) minimum daily temperature (see Table 1 for all index definitions).

2.3.2 Temperature extremes

To capture exceptional hot temperature, we quantified the annual number of warm and extreme warm days as TX95p and TX99p (in days per year), which is the annual count of days when Tmax ≥ 95th or 99th percentile of the 1960–2020 daily measured Tmax record. We quantified the number of warm and extreme warm nights as TN95p and TN99p (in nights $year^{-1}$), which is the annual count of nights when Tmin ≥ 95th or 99th percentile of the 1960–2020 daily measured Tmin record. To capture exceptional cold temperature, we quantified the number of cool and extreme cool days as TX5p and TX1p (in days $year^{-1}$), which is the annual count of days when Tmax ≤ 95th or 99th percentile of the 1960–2020 daily measured Tmax record. We quantified the number of cool and extreme cool nights as TN5p and TN1p (in nights), which is the annual count of nights when Tmin ≤ 95th or 99th percentile of the 1960–2020 daily measured Tmin record.

2.3.3 Rainfall

To quantify rainfall, we considered annual total precipitation (PTOT, in mm), annual dry season precipitation (PDRY, in mm), and annual wet season precipitation (PWET, in mm). Dry season months are defined as those with median precipitation below the overall 1960–2020 median monthly precipitation (142 mm $month^{-1}$). Yangambi exhibits two dry seasons alternating with two rainy seasons (Supplementary Fig. 4). A long dry season extends from December to February, followed by a short rainy season from March to May. Then, a short dry season covering the months of June and July is followed by a long rainy season from August to November.

2.3.4 Rainy days

We first counted the annual total number of wet (or rainy) days (Rd, in days $year^{-1}$), with a wet day defined as a day with rainfall ≥ 1 mm. We then counted the number of wet days in the dry season (RdDRY) as the sum of long ($RdDRY_{djf}$) and short ($RdDRY_{jj}$) dry season rainy days. Finally, we counted the number of wet days in the wet season (RdWET) as the sum of short ($RdWET_{mam}$) and long ($RdWET_{ason}$) wet season rainy days.

2.3.5 Rainfall intensity

To quantify rainfall intensity, we calculated the annual average rainfall from wet days, known as the simple day intensity index (SDII, in mm). We also calculated dry (SDII_DRY) and wet (SDII_WET) season simple day intensity index. To quantify extreme precipitation, we considered indices based on the 95th and 99th percentiles, where R95p is the annual count of days when daily rainfall ≥ 95th percentile of the 1960–2020 daily rainfall record and R99p is the annual count of days when daily rainfall ≥ 99th percentile of the 1960–2020 daily rainfall record. R95p and R99p (in days) represent the number of very wet days and extreme wet days respectively. Derived indices are R95pSUM which is the annual precipitation (in mm) from days when rainfall ≥ 95th mm percentile of the 1960–2020 daily rainfall record and R99pSUM which is the annual precipitation (in mm) from days when rainfall ≥ 99th mm percentile of the 1960–2020 daily rainfall record. R95pSUM and R99pSUM (in mm) represent very wet day intensity and extreme rainfall intensity respectively. Finally, we considered R95pTOT which is the percentage of annual precipitation from days when rainfall ≥ 95^{th} percentile of the 1960–2020 daily rainfall record and R99pTOT which is the percentage of annual precipitation from days when rainfall ≥ 99th percentile. R95pTOT and R95pTOT (in %) represent the very wet day proportion and extreme rainfall proportion respectively.

2.3.6 Water demand and availability

Potential evapotranspiration (PET) is a widely used indicator of the environmental demand for evapotranspiration (Tadese et al. 2020). Here, we calculate PET using Hamon's equation (Lu et al. 2005):

$$\mathrm{PET} = 0.1651 \times \mathrm{Ld} \times 216.7 \times \mathrm{ESAT}/(\mathrm{ATM} + 273.3)$$

where ATM is the annual average of the daily mean temperature (in °C), Ld is the day length (almost constantly 12 h in Yangambi), and ESAT is the saturation vapor pressure:

$$\mathrm{ESAT} = 6.108 \times \mathrm{EXP}(17.26939 \times \mathrm{ATM}/(\mathrm{ATM} + 237.3))$$

Furthermore, we calculated net water available (NWA) as follows (Tadese et al. 2020):

$$\mathrm{NWA} = \mathrm{PTOT} - \mathrm{PET}$$

NWA is a measure for the water available for runoff, tissue storage, soil moisture, and groundwater recharge.

2.3.7 Drought and seasonality indices

We calculated annual maximum climatic water deficit (MCWD), which is a commonly used metric of dry season intensity that has been widely applied in analysis of tropical forest responses to climate change (Aragão et al. 2014; Aguirre-Gutiérrez et al. 2020; Bennett et al. 2021). First, we calculated monthly climatic water deficit (CWD) values for each subsequent series of 12 months (complete years). Monthly CWD estimation begins with the wettest month of the first year in the record and is calculated as monthly evapotranspiration (ET_i) minus monthly precipitation (P_i) (Hubau et al. 2020; Bennett et al. 2021). ET_i is calculated from monthly PET_i and P_i using a simple model calibrated using the global

eddy covariance flux network and remote sensing data (Sun et al. 2011; Sun 2013; Fang et al. 2016):

$$\mathrm{ET_i} = 19.86 + 0.77 * \mathrm{PET} - 0.04 \times P_i$$

Then, CWD values for the subsequent 11 months were calculated recursively as:

$$\mathrm{CWD}_i = \mathrm{ET}_i - P_i + \mathrm{CWD}_{i-1}$$

where negative $\mathrm{CWD_i}$ values were set to zero (no drought conditions). This procedure was repeated for each subsequent complete 12 months. We then calculated the annual MCWD as the largest monthly CWD value for every complete year within the record. Larger MCWD indicates more severe water deficits.

Finally, we calculated the seasonality index (SI) for each year in the record as (Walsh and Lawler 1981):

$$SI_i = 1/R_i \times \sum_{n=1}^{n=12} \left(X_{in} - R_i/12\right)$$

where R_i is the total annual precipitation for the particular year i and X_in is the actual monthly precipitation for month n. The seasonality index allows classifying climate based on rainfall seasonality using the following categories:

SI < 0.19: precipitation spread throughout the year
SI = 0.20–0.39, precipitation spread throughout the year but with a definite wetter season; SI = 0.40–0.59, rather seasonal climate with a short dry season; SI = 0.60–0.79, seasonal climate; SI = 0.80–0.99, marked seasonal climate with a long dry season; SI = 1.00–1.19, most precipitation in < 3 months

2.4 Linear regression analysis

2.4.1 Long-term linear trends

To analyze long-term linear trends over the entire 1960–2020 dataset, we fitted linear mixed models on the daily and monthly meteorological indices from the Yangambi climate station, following Bush et al. (2020). For temperature indices (ATN and ATX) and SDII, we used a linear mixed effect model via REML (lmer command) from the lme4 R package (Bates et al. 2015). For rainfall (PTOT, Rd) indices, we fitted compound Poisson generalized linear mixed models (cpglmm command) from the cplm R package (Zhang 2013). The cpglmm models are exponential dispersion models using true likelihood-based inferential procedures (i.e., the Laplace approximation and the adaptive Gauss-Hermite quadrature). They are recommended for (positive and continuous) daily or monthly rainfall data which typically contain many zeros (Hasan and Dunn 2010). The lmer and cpglmm models regress the response variable against the year as predictor and include a random effect to account for seasonality and the hierarchical structure of the data. In the models using daily data, day-of-the-year was included as a random effect, that is, by assuming that the intercept can vary randomly among the days of the year. In the models on monthly data, we used month-of-the-year as a random effect. To evaluate the meaningfulness of the slope in the models, we compared model AIC with that of an intercept-only model (representing no long-term

change). If AIC of the model with slope is lower than that of the intercept-only model, we consider the slope significant. To evaluate seasonal trends, models were also run on dry season and wet season subsets of the daily and monthly rainfall indices (PDRY, PWET, SDII_DRY, SDII_WET, RdDRY, RdWET).

Additionally, we performed the nonparametric Kendall's tau test on the yearly meteorological indices to determine if the monotonic long-term linear trend in the time series was significant. We performed Kendall's test on smoothed time series using locally weighted regression (lowess filter) following Peterson et al. (2008). Kendall's tau test has been widely used to compute trends in hydrometeorological series because it is robust to the effect of outliers in the series (Peterson et al. 2008; Aguilar et al. 2009; Chaney et al. 2014). We performed smoothing using the lowess function of the gplot package (Cleveland 1979) and we performed Kendall's test using the kendallTrendTest function of the EnvStats package in R (Kendall 1975).

2.4.2 Piecewise linear trends

To analyze short-term trends within the 1960–2020 dataset, we fitted linear breakpoint models on the yearly meteorological indices from the Yangambi climate station. We first smoothed each annual index using the rollmean function of the zoo package in R with a 5-year moving-average window. Then, we parameterized a simple linear regression model on the full time series using the lm function in R. Finally, for each index, we parameterized single breakpoint and double breakpoint models using the segmented package in R (Muggeo 2008). For the single breakpoint models, we specified 1990 as the initial breakpoint value; for the double breakpoint models, we specified 1980 and 2000 as initial breakpoints. Starting from these, the segmented function then estimates best-fit breakpoints using the bootstrap restarting algorithm (Wood 2001).

To select the best-fit model for each index, we considered the R^2 value and the P-value of the Davies test (using the Davies test function of the segmented package). The Davies test allows to evaluate whether a model would be significantly improved when adding an extra breakpoint (Davies 2002). Specifically, if the P-value of the Davies test (P_{davies}) for a certain model is < 0.05, then the model would be improved by allowing another breakpoint.

For each index, we started by considering the simplest model. We selected the non-breakpoint model if its $P_{\text{davies}} > 0.05$ and $R^2 > 0.2$. Then, if the non-breakpoint model was rejected based on one or both of these criteria, we selected the single breakpoint model if its $P_{\text{davies}} > 0.05$ and $R^2 > 0.2$, and if the model converged. Then, if the single breakpoint model was rejected based on these criteria, we selected the double breakpoint model if it converged.

Additionally, we considered the meaningfulness of the breakpoints for selected double breakpoint models. If the two breakpoints were less than 5 years apart, the double breakpoint model was rejected in favor of the single breakpoint model. Supplementary Table 1 shows the slope(s), intercept(s), P-value(s), and breakpoint(s) for the selected model for each index. Slopes with a P-value < 0.05 are considered significant.

2.5 Comparison with gridded datasets

To compare the long-term rainfall trends observed in the Yangambi record, we used two gridded monthly rainfall datasets. We extracted Yangambi rainfall data from the Global Precipitation Climatology Centre (GPCC) at 1° resolution (~3025 km^2) (Schneider et al. 2014). We used the GPCC's most accurate in situ land surface precipitation analysis product by combining the Full Data V7 Product (1901–2010), based on quality-controlled data from 67,200 meteorological stations worldwide that feature record durations of 10 years or longer, with the V6 monitoring product (2011–2014), based on quality-controlled data from 7000 stations. This resulted in a GPCC rainfall record covering 1960–2014. Second, we extracted Yangambi rainfall data from the 0.25° resolution (~757 km^2) data from the Tropical Rainfall Measurement Mission (TRMM product 3B43 V7) from 1998 to 2020 (Huffman et al. 2007) which provides up-to-date satellite data for the whole tropical realm. Because TRMM only starts at 1998, we combined it with GPCC, following Hubau et al. (2020) and Bennett et al. (2021). The fit for the overlapping time period (1998–2014) was used to correct any systematic difference between GPCC and TRMM (Hubau et al. 2020). This resulted in a TRMM-GPCC rainfall record covering 1960–2020. GPCC and TRMM are the most widely used benchmark datasets to validate other gridded rainfall datasets (Nicholson et al. 2018b; Sun et al. 2018; Harris et al. 2020; Igri et al. 2022; Ndehedehe and Agutu 2022) and to analyze tropical forest responses to climate change (Zhou et al. 2014; Hubau et al. 2020; Bennett et al. 2021).

To compare the long-term temperature trends observed in the Yangambi record, we extracted monthly mean temperature from the Climatic Research Unit (CRU TS version 4.03; ~3025 km^2 resolution; released 15 May 2019; https://crudata.uea.ac.uk/cru/data/hrg/ (Harris et al. 2020).

Comparing observed (Yangambi) and extracted (CRU, GPCC, TRMM) data is a symmetric problem, meaning that we have a pair of Y variables and we want to see how they are related to each other. We therefore performed standardized major axis estimation using the sma command of the smart package in R (Warton et al. 2012). We used robust estimation to ensure that inferences are valid in the presence of outliers, which exist in all these databases.

3 Results

3.1 Long-term linear trends

We find a significant long-term increase in minimum (ATN), mean (ATM), and maximum (ATX) daily temperature, at 0.14, 0.18, and 0.21 °C per decade respectively, using the daily Yangambi climate station data (Table 2). This is confirmed using the monthly (Table 3) and yearly (Table 4) meteorological indices. We also find a long-term significant increase in (extreme) warm nights and (extreme) warm days and a significant decrease in (extreme) cool days (Table 4). All temperature indices reached record breaking values during the last few years (Fig. 2). ATX and ATN reached absolute maxima in respectively 2016 and 2020. ATX increased by 1.6 °C (from 29.2 to 30.8 °C) and ATN by 1.4 °C (from 19.8 to 21.2 °C) since the 1960s. Similarly, the number of warm days (TX95p) and warm nights (TN95p) also peaked in 2016 and 2020, at 46 and 118 days/nights per year respectively. To compare, 1960 only had 2 warm days and 4 warm

nights. Finally, the number of cool days (TX5p) decreased to a minimum of 11 per year in 2016 and the number of cool nights (TN5p) decreased to zero in 2019.

We do not find a significant long-term change in total annual precipitation (PTOT) using the daily and monthly data, although the difference in AIC between the slope and the no-slope models is very small ($\Delta AIC < 2$; Table 2 and Table 3). However, Kendall's tau test using annual data smoothed by the lowess model shows contrasting long-term slopes between dry season precipitation (PDRY; decreasing at − 5 mm per year per decade; $P = 0.009$) and wet season precipitation (PWET; increasing at 17 mm per year per decade; $P < 0.001$) (Table 4). Declining dry season precipitation and increasing wet season precipitation suggest an increasing precipitation seasonality trend in Yangambi (Fig. 2, Table 4). This is confirmed by long-term trends in net water availability (NWA), a metric that accounts for both precipitation and temperature. NWA is declining significantly in the dry season (NWA_DRY, at − 10.56 mm per year per decade) and increasing significantly in the wet season (NWA_WET, at 8.5 mm per year per decade) (Table 4).

Using the monthly and yearly data, we find a significant long-term decrease in the yearly number of rainy days (Rd, at − 2.8 days per year per decade) and a significant increase in rainfall intensity, with a simple day intensity index (SDII) increasing at 0.48 mm per day per decade (Table 3, Table 4). This is confirmed by significant increases in very wet day frequency, intensity, and proportion (R95p, R95pSUM, R95pTOT; see Table 1 for index

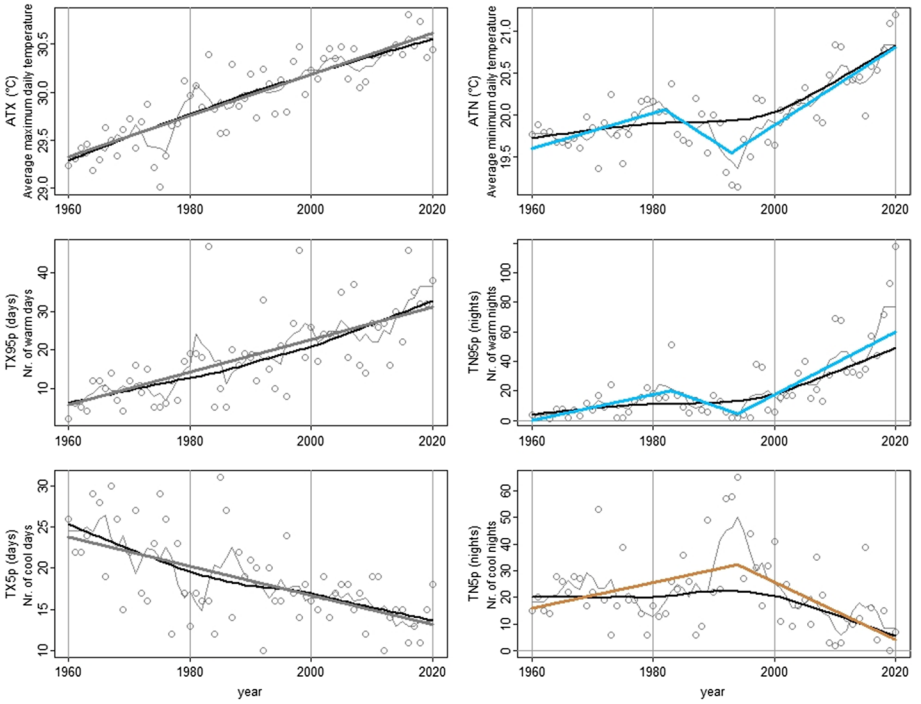

Fig. 2 Patterns of temperature and temperature extreme indices in Yangambi, measured over the period 1960–2020. Each open circle represents one yearly record; the thin gray line shows the smoothed 5-year moving-average time series; the thick solid black line shows the lowess smoother (slopes and *P*-values in Table 4). Thick colored lines represent best-fit linear regression models (non-breakpoint models in gray, single breakpoint models in orange, double breakpoint models in blue). Regression lines are solid if significant or dashed if non-significant. Index definitions are given in Table 1; slopes and *P*-values of breakpoint regression models are given in Supplementary Table 1

definitions) and extreme rainfall frequency, intensity, and proportion (R99p, R99pSUM, R99pTOT). The number of rainy days is decreasing both in the dry and wet seasons (Rd_DRY and Rd_WET), and rainfall intensity is increasing in both dry and wet seasons (SDII_DRY and SDII_WET). This suggests that precipitation intensity is increasing throughout the year.

3.2 Piecewise trends: temperature

Selected simple linear models vary among temperature indices. For ATX, the non-breakpoint model is selected, while for ATN and ATM, the double breakpoint model was selected (Supplementary Table 1, Fig. 2). Using the simple regression model, ATX increased significantly ($P < 0.001$) and continuously over the full 1960–2020 period, at 0.22 °C per decade, which is comparable to the linear mixed models on the daily (Table 2) and monthly (Table 3) data. ATN and ATM both initially show an increase, then a significant decrease between 1982 and 1993, and finally a very steep, nearly three-decade increase from 1993 until 2020, at 0.47 and 0.34 °C per decade for ATN and ATM respectively (all trends significant with $P < 0.001$) (Fig. 2).

Selected simple linear models also vary among night-time extreme temperature indices (Supplementary Table 1, Fig. 2). Single breakpoint models were selected for the number of cool nights (TN5p) and extreme cool nights (TN1p). These indices increased in the first half of the record, but decreased significantly at the end of the record (all trends significant with $P < 0.001$). Especially, the number of extreme cool nights (TN1p) decreased spectacularly since 1994, at − 10.8 nights per decade. In contrast, the number of extreme warm nights (TN99p) increased continuously and significantly ($P < 0.001$) throughout the 1960–2020 record, at 1.8 nights per decade. A double breakpoint model was selected for the number of warm nights (TN95p), with a spectacular increase since 1994, at 2.1 nights per decade (Fig. 2).

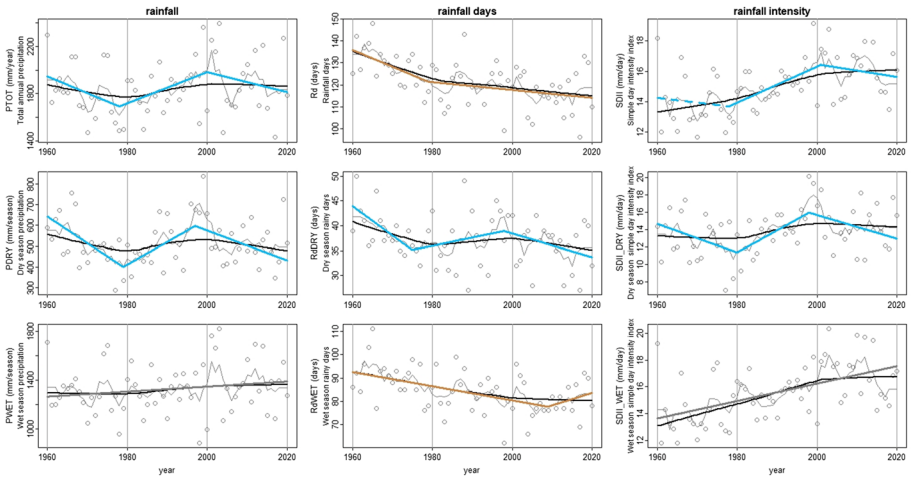

Fig. 3 Patterns of precipitation (dry and wet season), rainy days, and rainfall intensity in Yangambi, measured over the period 1960–2020. Figure details as in Fig. 2

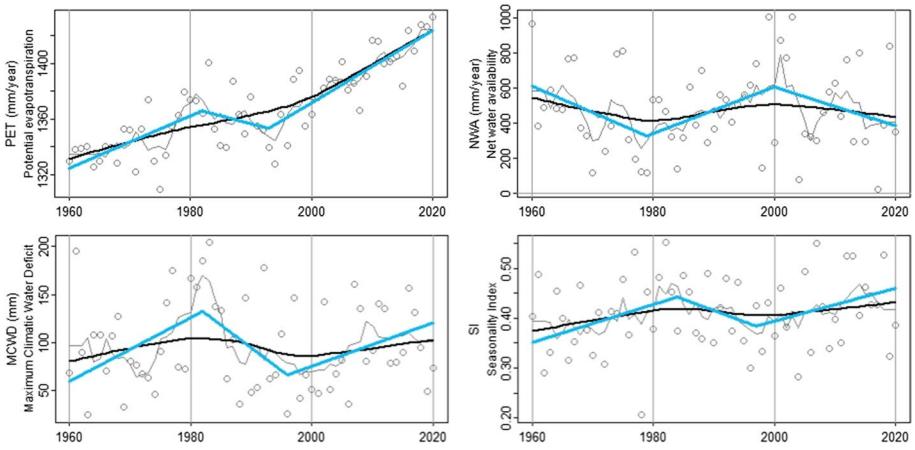

Fig. 4 Patterns of water demand (PET), net water availability (NWA), maximum climatic water deficit (MCWD), and seasonality (SI) in Yangambi, measured over the period 1960–2020. Figure details as in Fig. 2

Selected simple linear models are remarkably comparable among extreme day-time temperature indices. For each of the indices, the non-breakpoint model was selected. The numbers of cool days (TX5p) and extreme cool days (TX1p) are significantly decreasing throughout the record, at − 1.8 and − 0.6 days per decade respectively ($P < 0.001$ for both indices; Supplementary Table 1). In contrast, we observe a consistent increase in warm days (TX95p) and extreme warm days (TX99p), at 4.2 and 1.3 days per decade respectively ($P < 0.001$ for both indices; Supplementary Table 1).

3.3 Piecewise trends: rainfall

Although precipitation indices do not show long-term trends (Table 2, Table 3), they do show significant short-term trends (Supplementary Table 1, Fig. 3). Total annual precipitation (PTOT), total annual number of rainfall days (Rd), and simple day intensity index (SDII) show remarkably similar breakpoints, around 1978 (all three indices) and around 2000 (PTOT, SDII) (Fig. 3), dividing the record in three almost equally long two-decade periods. The first period (1960–1978) is characterized by decreasing precipitation (PTOT, $P = 0.001$), decreasing number of rainy days (Rd, $P < 0.001$), and no change in rainfall intensity (SDII, $P = 0.296$) (Supplementary Table 1). The second period (1979–1999) is characterized by increasing precipitation (PTOT, $P < 0.001$), decreasing rainy days

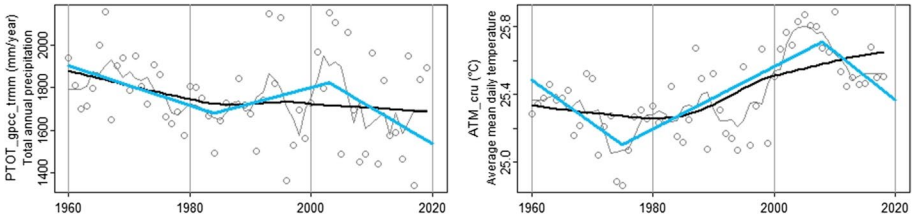

Fig. 5 The precipitation record extracted from GPCC (1960–1997) and TRMM (1998–2020) for Yangambi and the annual average mean daily temperature record extracted from CRU. Figure details as in Fig. 2

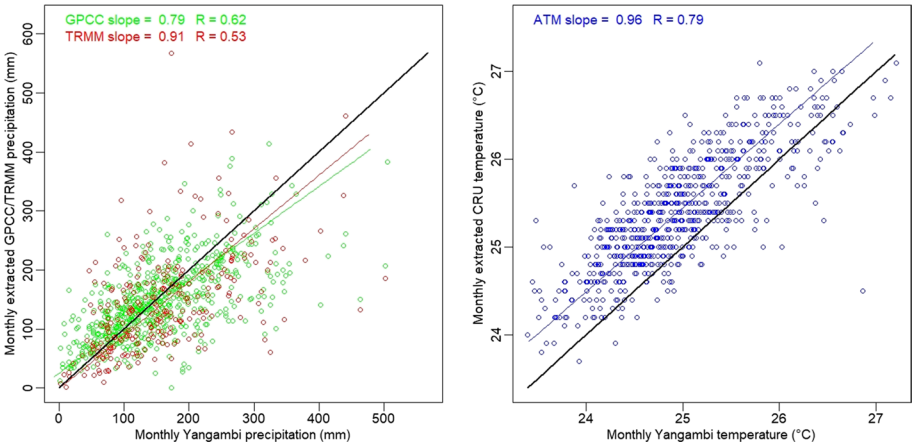

Fig. 6 Comparison between observed records of precipitation and temperature from the Yangambi meteorological station with those from existing gridded datasets. Scatterplots show observed (*x*-axis) monthly precipitation and mean temperature observations from the Yangambi record (1960–2020) versus extracted observations for the same months from GPCC (green, 1960–2014), TRMM (red, 1998–2019), and CRU (blue, 1960–2019). Colored lines represent standardized major axis estimation models; correlation coefficients (*R*) and slopes are shown in the top right corner. The 1:1 line is shown in black

(Rd, $P<0.001$), and increasing rainfall intensity (SDII, $P<0.001$). The third period (2000–2020) is characterized by decreasing precipitation (PTOT, $P=0.001$), decreasing number of rainy days (Rd, $P<0.001$), and decreasing rainfall intensity (SDII, $P<0.001$).

Furthermore, trends are remarkably different among the seasons. The wet season is characterized by a significant long-term increase in total precipitation (PWET, $P=0.013$) and rainfall intensity (SDII_WET, $P<0.001$), along with a decrease in rainy days (Rd_WET, $P<0.001$) (Supplementary Table 1, Fig. 3). Also, very wet day frequency (R95p) and proportion (R95pTOT) are increasing throughout the record (Supplementary Table 1). In contrast, the dry season is characterized by two-decadal trends that are very similar to full-year trends. Specifically, dry season precipitation (PDRY), number of rainfall days (Rd_DRY), and simple day intensity index (SDII_DRY) are decreasing from 1960 to 1979 (breakpoint varies between 1975 and 1980 among indices). Then, all indices are increasing from 1980 to 1998 and decreasing again from 1999 to 2020 (Supplementary Table 1; all $P<0.001$).

3.4 Piecewise trends: drought and seasonality

The short-term trends observed in the full-year and dry season records are also reflected in the standardized precipitation evapotranspiration index (SPEI) (Vicente-Serrano et al. 2010), which is mathematically similar to the standardized precipitation index (SPI), but it includes the role of temperature. We counted the frequency of dry months by decade in the Yangambi precipitation record, using well-defined drought categories (Supplementary Table 2 and Supplementary Fig. 5). We find that the 1960s had a very low number of dry months in all categories (12%), followed by the 1970s which had a slight increase in dry months (15%); the 1980s and 2010s had a moderately high number of dry months

respectively (17% in each of the two decades); and finally, the 1990s and 2000s had a very high number of dry months (19% in each of the two decades). This indicates a wetting trend from 1960 to 1970, an increasing trend to moderate drought observed in the 1980s and 2010s, and then a trend to very high drought from 1990s to 2000s.

A drought index based on both mean annual temperature (ATM) and total annual precipitation (PTOT) is net water availability (NWA) (Tadese et al. 2020). NWA is the balance between total water availability (precipitation, PTOT) and water demand (expressed as potential evapotranspiration, PET, which is calculated as a function of ATM). We find that both full-year and dry season patterns in NWA are very similar to those of PTOT (Supplementary Table 1, Fig. 4). Dry season NWA was negative (indicating water shortage) during most periods in the record, except the 1960s and 1990s (Supplementary Table 1). In contrast, wet season NWA was always positive and increased throughout the 1960–2020 record ($P = 0.044$), while dry season NWA decreased, increased, and decreased again during subsequent two-decadal periods (all $P < 0.001$).

The rainfall (Fig. 3) and drought (Fig. 4) trends show substantial differences between the dry and wet season. This suggests shifts in precipitation seasonality across the record. To test this, we finally assessed trends in two rainfall seasonality indices: the Walsh and Lawler seasonality index (SI) and the maximum climatological water deficit (MCWD) (Fig. 4, Supplementary Table 1). For both indices, the double breakpoint model was retained, again with breakpoints close to those in the PTOT model, dividing the record in three nearly two-decadal periods. We find that seasonality was significantly increasing, then decreasing, and finally increasing again (all $P < 0.001$). The seasonality index indicates that the precipitation regime in Yangambi switched between two different categories over the 1960–2020 period. In the wettest decades (1960s and 1990s), SI reached minima of 0.28 and 0.29 (in 1962 and 1996), which indicates that "precipitation was spread throughout the year" (Walsh and Lawler 1981). In the driest decade (1980s), SI reached a maximum of 0.55, which indicates a "rather seasonal precipitation regime." The last two decades also tended to be rather seasonal, with an average SI of 0.40 and 0.44 and a maximum SI of 0.53 (2012 and 2018).

3.5 Comparison with gridded datasets

The combined GPCC (1960–1997) and TRMM (1998–2020) precipitation record shows a significant declining long-term trend from 1960 to 2020, at − 50 mm per decade ($P < 0.001$), in contrast with a non-significant (Table 2, Table 3) or even slightly increasing (Table 4) long-term precipitation trend in the observed Yangambi record. However, piecewise regression in the GPCC-TRMM record for Yangambi shows a declining (1960–1984), then increasing (1985–2003), and again declining (2004–2020) trend (blue lines in Fig. 5). This piecewise pattern is similar to the observed piecewise trends (Fig. 3).

The annual average mean daily temperature record extracted from CRU shows a non-significant long-term trend ($P = 0.298$), in contrast with a significant warming trend in the observed Yangambi record (Table 2, Table 3, Table 4). Piecewise regression in the CRU record does show a significant warming trend between 1975 and 2008, but a drop during the last decade (Fig. 5), which contrasts with a consistent steep warming trend in the observed record since 1995 (Fig. 2).

Slopes of standardized major axis estimation models are close to 1, suggesting good agreement between the observed and extracted monthly precipitation values, for GPCC (slope = 0.79), TRMM (slope = 0.91), and CRU (slope = 0.96) (Fig. 6). This indicates that

Table 1 Index categories and definitions

Index category	Symbol	Definition
Temperature	ATX	Annual average maximum daily temperature
	ATM	Annual average mean daily temperature
	ATN	Annual average minimum daily temperature
Temperature extremes	TN1p	Number of extreme cool nights—annual nr of nights when Tmin ≤ 1th percentile of 1960–2020
	TN5p	Number of cool nights—annual number of nights when Tmin ≤ 5th percentile of 1960–2020
	TN95p	Number of warm nights—annual number of nights when Tmin ≥ 95th percentile of 1960–2020
	TN99p	Number of extreme warm nights—annual nr of nights when Tmin ≥ 99th percentile of 1960–2020
	TX1p	Number of extreme cool days—annual nr of days when Tmax ≤ 1th percentile of 1960–2020
	TX5p	Number of cool days—annual number of days when Tmax ≤ 5th percentile of 1960–2020
	TX95p	Number of warm days—annual number of days when Tmax ≥ 95th percentile of 1960–2020
	TX99p	Number of extreme warm days—annual nr of days when Tmax ≥ 99th percentile of 1960–2020
Rainfall	PTOT	Total annual precipitation
	PDRY	Dry season precipitation
	PWET	Wet season precipitation
	Rd	Rainfall days, i.e., annual total number of wet days (rainfall ≥ 1 mm)
	RdDRY	Dry season rainy days
	RdWET	Wet season rainy days

Table 1 (continued)

Index category	Symbol	Definition
Rainfall intensity	SDII	Simple day intensity index: average rainfall from wet days (rainfall ≥ 1 mm)
	SDII_DRY	Dry season simple day intensity index
	SDII_WET	Wet season simple day intensity index
	R95p	Very wet day frequency, i.e., annual number of days when rainfall ≥ 95th percentile of the 1960–2020 daily rainfall record
	R99p	Extreme rainfall frequency, i.e., annual number of days when rainfall ≥ 99th percentile of the 1960–2020 daily rainfall record
	R95pSUM	Very wet day intensity, i.e., total annual precipitation from days when rainfall ≥ 95th mm percentile for 1960–2020
	R99pSUM	Extreme rainfall intensity, i.e., total annual precipitation from days when rainfall ≥ 99th mm percentile for 1960–2020
	R95pTOT	Very wet day proportion, i.e., percentage of annual precipitation from days when rainfall ≥ 95th percentile of 1960–2020
	R99pTOT	Extreme rainfall proportion, i.e., percentage of annual precipitation from days when rainfall ≥ 99th percentile of 1960–2020
Seasonality	MCWD	Maximum climatic water deficit
	SI	Seasonality Index
Water demand and availability	PET	Potential evapotranspiration
	PET_DRY	Dry season potential evapotranspiration
	PET_WET	Wet season potential evapotranspiration
	NWA	Net water availability
	NWA_DRY	Dry season net water availability
	NWA_WET	Dry season net water availability

Table 2 Comparisons of linear regression model results to test for long-term trends in temperature and rainfall indices using "daily" observations from the Yangambi meteorological station (1960–2020). We used linear mixed models (lmer) for temperature indices and compound Poisson generalized linear mixed models cpglmm) for precipitation. For each model, day-of-the-year was included as a random intercept to account for seasonality and the hierarchical structure of the data. For each index, we ran a model without slope (representing no long-term change) and a model with a slope. Here, we present AIC of each model and the difference (ΔAIC) between both models. For each index, the model with lowest AIC is retained (indicated in bold)

Index	AIC_no_slope	AIC_slope	Δ AIC	Slope	Slope unit
ATN	68,195.9	**67,110.1**	**−1085.9**	**0.14**	°C decade^{-1}
ATM	74,707.9	**73,442.7**	**−1265.2**	**0.18**	°C decade^{-1}
ATX	99,425.1	**98,855.1**	**−570.0**	**0.21**	°C decade^{-1}
PTOT	**97,325.3**	97,327.0	1.6	9.34	mm decade^{-1}
PDRY	**33,184.0**	33,186.0	1.9	−1.83	mm decade^{-1}
PWET	**63,894.3**	63,895.3	1.0	13.52	mm decade^{-1}

high observed values generally correspond to high extracted values. However, moderate correlation coefficients ($R=0.62$ for GPCC, $R=0.53$ for TRMM) suggest that absolute monthly precipitation values are sometimes very different between the extracted and observed data, although differences exist in both ways (sometimes observed values are higher than extracted values and vice versa). For CRU, the correlation coefficient is high ($R=0.79$) but extracted values from CRU tend to be systematically higher than observed values in Yangambi, in the order of ~0.5 °C.

4 Discussion

4.1 Consistent warming trend

Long-term continuous warming over the entire 1960–2020 period in Yangambi (Table 2, Table 3, Table 4) is consistent with the overall temperature change in Western and Central Equatorial Africa, where ATM has increased by about 1 °C in the past 70 years (Dezfuli and Dezfuli 2017). Increasing numbers of (extreme) warm days and nights and decreasing numbers of (extreme) cool days and nights are consistent with reported changes in temperature extremes throughout Central Africa since 1955 (Aguilar et al. 2009; Chaney et al. 2014).

4.2 Contrasting regional long-term precipitation trends

The non-significant long-term precipitation trend in Yangambi (Table 2, Table 3) corroborates a non-significant trend over the 1979–2005 period in the same region (Chaney et al. 2014). The short-term decline in PTOT observed in Yangambi between 1960 and 1980 corresponds to a reported continuous rainfall decline over most of the Central African continent, as indicated by analysis of all available gauge stations during that time period (Nicholson et al. 2018a). One of the wettest years in the overall central African gauge station network is 1961, whereas 1983 is among the driest years (Nicholson et al. 2018b).

Table 3 Comparisons of linear regression model results to test for long-term trends in temperature and rainfall indices using "monthly" indices calculated from the Yangambi meteorological station data (1960–2020). We used linear mixed models (lmer) for temperature and SDII indices. We used compound Poisson generalized linear mixed models (cpglmm) for precipitation and Rd. For each model, month-of-the-year was included as a random intercept to account for seasonality and the hierarchical structure of the data. For each index, we ran a model without slope (representing no long-term change) and a model with a slope. Here, we present AIC of each model and the difference (ΔAIC) between both models. For each index, the model with lowest AIC is retained (indicated in bold)

Index	AIC_no_slope	AIC_slope	Δ AIC	Slope	Slope unit
ATN	1294.4	**1152.1**	**−142.3**	**0.14**	°C decade^{-1}
ATM	1132.0	**805.6**	**−326.4**	**0.18**	°C decade^{-1}
ATX	1464.5	**1177.4**	**−287.1**	**0.21**	°C decade^{-1}
PTOT	**7979.4**	7980.9	1.5	12.01	mm decade^{-1}
PDRY	**3190.7**	3192.7	2.0	−1.04	mm decade^{-1}
PWET	**4774.5**	4775.6	1.1	13.22	mm decade^{-1}
SDII	4501.4	**4487.6**	**−13.8**	**0.48**	mm day^{-1} decade^{-1}
SDII_DRY	1925.8	**1924.5**	**−1.3**	**0.38**	mm day^{-1} decade^{-1}
SDII_WET	2559.2	**2546.4**	**−12.8**	**0.56**	mm day^{-1} decade^{-1}
Rd	3541.4	**3527.6**	**−13.8**	**−2.84**	days month^{-1} decade^{-1}
RdDRY	1186.9	**1186.0**	**−0.9**	**−0.77**	days month^{-1} decade^{-1}
RdWET	2066.8	**2055.1**	**−11.8**	**−2.07**	days month^{-1} decade^{-1}

The short-term increase in PTOT in Yangambi between 1981 and 1999 is also prominent in the interpolated central African gauge dataset, where 1997 is among the wettest years (Nicholson et al. 2018b). Finally, the declining trend in PTOT in Yangambi between 2000 and 2020 corroborates previous reports of significant drying in the Congo Basin during the past two decades (Malhi and Wright 2004; Asefi-Najafabady and Saatchi 2013; Diem et al. 2014; Zhou et al. 2014; Tsalefac et al. 2015; Dezfuli and Dezfuli 2017; Nicholson et al. 2018b, 2019; Mabrouk et al. 2022).

We note substantial similarities between our observed piecewise trends in PTOT and piecewise trends in published Congo River's annual discharge data (Mahé 1995; Laraque et al. 2013, 2020; Tsalefac et al. 2015; Bola et al. 2022; Ndehedehe and Agutu 2022) (Supplementary Fig. 6). Nevertheless, we also note substantial differences in long-term trends, with significant decline in Congo River's discharge since 1960 versus no significant change in PTOT in Yangambi. This is due to the historically high Congo River discharge levels in the 1960s, which must be related to anomalously high precipitation in regions within the Congo Basin other than the Yangambi region. Similarly, the precipitation pattern in Yangambi contrasts with the strong negative continuous drying trend at −75 mm per decade over the 1984–2018 period in the Lopé National Park (Gabon) (Bush et al. 2020). Furthermore, it contrasts with strong negative rainfall trends over the northern and southern sector of the Congo Basin (Dezfuli and Dezfuli 2017) and a significant negative trend at −31 mm per year per decade (Aguilar et al. 2009) over the 1955–2003 period in the entire central Congo Basin. This confirms strong differences in long-term precipitation trends among central African regions (Dezfuli and Dezfuli 2017). Indeed, recent analysis of gridded products (GPCC and CRU) showed remarkable spatial variability in precipitation change across the entire Congo Basin, with two-decadal trends (decreasing precipitation in 1961–1980, increase in 1981–2000, decrease in 2001–2013) for the Yangambi area similar to those observed in our record (Ndehedehe and Agutu 2022).

Table 4 Comparisons of linear regression model results to test for long-term trends in temperature and rainfall indices using "yearly" indices calculated from the Yangambi meteorological station data (1960–2020). For each index, we performed a nonparametric test for a monotonic trend based on Kendall's tau statistic, using yearly data smoothed with the lowess function. Significant indices ($P < 0.05$) are highlighted in bold

Index category	Index	Kendall's tau	*P*-value (Kendall)	Slope (Kendall)	Slope unit
Temperature	**ATX**	**1.00**	**< 0.001**	**0.21**	**°C decade^{-1}**
	ATM	**1.00**	**< 0.001**	**0.16**	**°C decade^{-1}**
	ATN	**1.00**	**< 0.001**	**0.12**	**°C decade^{-1}**
Temperature extremes	**TN1p**	**0.47**	**< 0.001**	**0.39**	**nights year^{-1} decade^{-1}**
	TN5p	− 0.17	0.052	− 1.03	nights year^{-1} decade^{-1}
	TN95p	**1.00**	**< 0.001**	**5.41**	**nights year^{-1} decade^{-1}**
	TN99p	**0.98**	**< 0.001**	**1.05**	**nights year^{-1} decade^{-1}**
	TX1p	**− 1.00**	**< 0.001**	**− 0.43**	**days year^{-1} decade^{-1}**
	TX5p	**− 1.00**	**< 0.001**	**− 1.65**	**days year^{-1} decade^{-1}**
	TX95p	**1.00**	**< 0.001**	**4.37**	**days year^{-1} decade^{-1}**
	TX99p	**1.00**	**< 0.001**	**1.10**	**days year^{-1} decade^{-1}**
Rainfall	**PTOT**	**0.33**	**< 0.001**	**11.28**	**mm year^{-1} decade^{-1}**
	PDRY	**− 0.23**	**0.009**	**− 5.05**	**mm year^{-1} decade^{-1}**
	PWET	**0.84**	**< 0.001**	**16.88**	**mm year^{-1} decade^{-1}**
	Rd	**− 1.00**	**< 0.001**	**− 2.40**	**days year^{-1} decade^{-1}**
	RdDRY	**− 0.56**	**< 0.001**	**− 0.63**	**days year^{-1} decade^{-1}**
	RdWET	**− 1.00**	**< 0.001**	**− 2.23**	**days year^{-1} decade^{-1}**

Table 4 (continued)

Index category	Index	Kendall's tau	*P*-value (Kendall)	Slope (Kendall)	Slope unit
Rainfall intensity	**SDII**	**1.00**	**< 0.001**	**0.50**	**mm day^{-1} decade^{-1}**
	SDII_DRY	**0.43**	**< 0.001**	**0.30**	**mm day^{-1} decade^{-1}**
	SDII_WET	**0.99**	**< 0.001**	**0.67**	**mm day^{-1} decade^{-1}**
	R95p	**0.72**	**< 0.001**	**0.68**	**days year^{-1} decade^{-1}**
	R99p	**0.65**	**< 0.001**	**0.51**	**days year^{-1} decade^{-1}**
	R95pSUM	**0.76**	**< 0.001**	**41.22**	**mm year^{-1} decade^{-1}**
	R99pSUM	**0.59**	**< 0.001**	**35.52**	**mm year^{-1} decade^{-1}**
	R95pTOT	**1.00**	**< 0.001**	**1.90**	**% decade^{-1}**
	R99pTOT	**0.62**	**< 0.001**	**1.76**	**% decade^{-1}**
Seasonality	MCWD	0.17	0.053	1.26	mm decade^{-1}
	SI	**0.63**	**< 0.001**	**0.01**	
Water demand and availability	**PET**	**1.00**	**< 0.001**	**12.78**	**mm year^{-1} decade^{-1}**
	PET_DRY	**1.00**	**< 0.001**	**4.92**	**mm year^{-1} decade^{-1}**
	PET_WET	**1.00**	**< 0.001**	**7.93**	**mm year^{-1} decade^{-1}**
	NWA	− 0.09	0.323	− 3.18	mm year^{-1} decade^{-1}
	NWA_DRY	**− 0.43**	**< 0.001**	**− 10.56**	**mm year^{-1} decade^{-1}**
	NWA_WET	**0.44**	**< 0.001**	**8.54**	**mm year^{-1} decade^{-1}**

4.3 Increasing precipitation "seasonality"

The increasing seasonality index (SI) and increasing maximum climatic water deficit (MCWD) over the 1998–2020 period (Fig. 4) suggest recent intensification of the seasonal rainfall cycle in Yangambi, with a drier dry season and wetter rainy season. This is confirmed by an increasing trend in wet season precipitation and a decreasing trend in dry season precipitation (Fig. 3). This trend towards intensifying precipitation seasonality in central Africa was recently confirmed by a combination of farmer perceptions, satellite-based estimates, and ground-based station measurements (Salerno et al. 2019).

Our observation of increasing long-term wet season precipitation in Yangambi is consistent with an observed spectacular increase in the annual lightning flash density and the number of stormy days in the central Congo Basin between 2005 (114 stormy days per year) and 2013 (189 stormy days per year) (Soula et al. 2016). Furthermore, our observation of a drying dry season over the last two decades (1999–2020) is consistent with the reported significant increase in dry season length in the Congo Basin, by 6.4–10.4 days per decade, attributed to an earlier dry season onset and a delayed dry season end (Jiang et al. 2019). Finally, it is consistent with an observed long-term (1982–2016) increase in the areal extent and intensity of thunderstorms over the Congo Basin, causing reduced moisture availability in the Lower troposphere over the Congo Basin (Raghavendra et al. 2018).

Opposing dry and wet season long-term precipitation trends in Yangambi (Table 4) are also comparable to the situation in Lopé (Gabon), where total precipitation decline was driven by a decline in rainfall in the long dry season (June–July–August-September) but not in the wet seasons. This suggests that increases in intra-annual rainfall variability, more specifically increased contrast between the wet and dry seasons, are a widespread phenomenon in Central Africa (Bush et al. 2020).

4.4 Increasing precipitation "intensity"

Our results (Table 4) also corroborate previously reported decrease in rainy days (at − 0.67 days per year per decade), a long-term increase in SDII (at 0.06 mm per day per decade), and increasing very wet day intensity in Central Africa (at 13.6 mm per year per decade) (Aguilar et al. 2009; Chaney et al. 2014). The combination of decreasing number of rainy days (Rd), increasing rainfall intensity (SDII), and increasing very wet day intensity (R95pSUM) confirms model outputs showing that wet extreme events are expected to become more frequent and more severe in Equatorial Africa (Fotso-Nguemo et al. 2018; Kendon et al. 2019; Karam et al. 2022).

4.5 Impact of climate variability in Yangambi

Continued warming and increasing precipitation seasonality and intensity in Yangambi (2000–2020) have a significant impact on local livelihoods. A recent study showed that the vast majority of farmers in Yangambi not only perceived changes in temperature and precipitation, but also experienced reduced crop yields and the emergence of new weed species and pests (Mangaza et al. 2021). Increasing impact of climate variability will particularly require implementation of climate-smart agriculture (Laux et al. 2010; Mangaza et al. 2021). Ongoing divergence of dry season (getting drier) and wet season (getting wetter and more intense) climate in Yangambi urges for a dynamic adaptation approach, where farmers introduce small management adjustments based on observed changes in

productivity in previous years, rather than following prescribed adjustment protocols (Meza and Silva 2009). The tangible impact of climate variability in Yangambi might also call for an increased focus on agroforestry, which is an example of a livelihood system combining various benefits and combining mitigation and adaptation effects (Batsi et al. 2020; Tschora and Cherubini 2020).

Finally, a shift towards a hotter and more seasonal climate may also have important consequences for Congo Basin forest composition and functioning. Several authors report ongoing shifts in species composition due to long-term drying in West Africa (Fauset et al. 2012; Aguirre-Gutiérrez et al. 2020) and in the drier parts of the Amazon (Esquivel-Muelbert et al. 2019). Dying wet-affiliated trees in the forest are replaced by more drought-tolerant (deciduous) species. No analysis using ground-based long-term forest inventory data has been conducted for Yangambi or any other region in the central Congo Basin yet, but analysis of satellite images revealed a long-term decline of Congo rainforest greenness, associated with a shift of species composition towards a larger proportion of deciduous species in the canopy (Zhou et al. 2014). Even though no shifts in forest composition have been reported for Yangambi through direct ground-based observations, increasing precipitation seasonality and decreasing net water availability are likely to lead to drought stress in its forests (Karam et al. 2022), which could push these ecosystems beyond their limits (James et al. 2013). Combined long-term and systematic monitoring of both biodiversity and climate in Yangambi and, more broadly, in the Congo Basin is indispensable to develop early warning systems for ecosystem degradation and collapse.

Our comparison analysis shows that remarkable discrepancies exist between observed climatic variables and those extracted from gridded products. Differences are found both in long-term trends and in absolute monthly values. Recent analysis showed that the correlation between observed and extracted (from TRMM) precipitation values is lowest in the wettest areas of central Africa (Igri et al. 2022). These results, combined with the exceptionally poor station network in the wet central Congo Basin, call for more intense efforts in climate monitoring.

5 Conclusions

Our newly digitized data from Yangambi represent a unique climate record in the central Congo Basin, a remarkably under sampled and hence enigmatic region in climate research. Our results from Yangambi corroborate recently reported long-term increase in temperature and temperature extremes throughout Central Africa since at least 1960. Short-term trends in the Yangambi records suggest that the increase in temperature and temperature extremes accelerated since the early 1990s. Our results show no long-term change in precipitation and drought indices in Yangambi. Nevertheless, we find long-term increasing intra-annual rainfall variability, both in terms of rainfall amount (decreasing the in dry season, increasing in the wet season) and in rainfall intensity (especially increasing in the wet season). Furthermore, we find highly significant short-term trends in precipitation and drought indices, dividing the record in three almost equally long two-decade periods. The first period (1960–1978) is characterized by decreasing precipitation, decreasing net water availability, and no change in rainfall intensity. The second period (1979–1999) is characterized by increasing precipitation, increasing net water availability, and increasing rainfall intensity. The third period (2000–2020) is characterized by decreasing precipitation, decreasing net water availability, and decreasing rainfall intensity. These short-term trends

are prominent in the dry season, but not in the wet season, which shows a significant long-term increase in precipitation, net water availability, and rainfall intensity. The seasonality index confirms that the precipitation regime in Yangambi switched between two different categories over the 1960–2020 period, from "rather seasonal" (1960–1978) to "precipitation spread throughout the year" (1979–1999) and back to "rather seasonal" (2000–2020).

Our results are in line with previous reports of a drying trend in the dry season in central Africa during the last two decades, based on available interpolated gridded climate datasets. Ongoing warming and increasing precipitation seasonality and intensity in Yangambi, with increasing extreme temperature events, drier dry seasons, and wetter rainy seasons, already have a significant impact on crop yields in Yangambi. This calls for urgent development of climate-smart and dynamic agriculture and agroforestry systems. To this end, systematic digitization and climate recording in the Congo Basin will be critical, especially because existing satellite and interpolated climate products are not entirely representative.

Supplementary Information The online version contains supplementary material available at https://doi.org/10.1007/s10584-023-03606-0.

Acknowledgements We sincerely thank all employees of the *Institut National pour la Recherche et l'Étude Agronomiques* (INERA), Yangambi (République Démocratique du Congo), particularly Lydie Mbambu Ketha, Bernard Ngutu Yebalemba, Jean-Marie Malite Atamba, Jean-Pierre Litonga Gelongo, Jean Bwailenge Lofole, and Pierre Ngaimoko Balemba, for daily observations and/or support for the digitization of data. This climatic record was established thanks to their persistent daily efforts. We thank Sharon Nicholson and Douglas Klotter for kindly providing the central African gauge station data from their publication (Nicholson et al. 2018b), reproduced in our Fig. 1. We thank Alain Laraque for helping us to obtain the Congo River discharge data used in Figure S5.

Author contribution Emmanuel Kasongo Yakussu, José Mbifo Ndiapo, Théophile Besango Likwela, Michel Lokonda Wa Kipifo, and Amand Mbuya Kankolongo led data collection. Emmanuel Kasongo Yakusu, Hans Beeckman, Nils Bourland, Françoise Gellens-Meulenberghs, Wannes Hubau, and Joris Van Acker conceived the study. Hans Beeckman, Nils Bourland, Jan Van den Bulcke, Joris Van Acker, Pascal Boeckx, Hans Verbeeck, and Kim Jacobsen secured the funding. Emmanuel Kasongo Yakusu digitized the data. Wannes Hubau and Emmanuel Kasongo Yakusu led data analysis, assisted by Hans Van de Vyver, Gaston Demarée, Françoise Gellens-Meulenberghs, and Marijn Bauters. Emmanuel Kasongo Yakusu and Wannes Hubau wrote the paper. All authors commented on the manuscript.

Funding The master and doctoral scholarships of E.K.Y. were financed by the European Union through the REFORCO, FCCC (Forêt et Changement Climatique au Congo), and FORETS (FOrmation, Recherche, Environnement dans la TShopo) projects, implemented by the Center for International Forestry Research (CIFOR) in collaboration with R&SD (Resources and Synergies Development) and Université de Kisangani. Scientific internship scholarships of E.K.Y. in Belgium were funded by the ABIC program of the Royal Museum for Central Africa (2016, 2017, 2018), by the COBECORE project, and by the PilotMAB project (June–November 2020), financed by the Direction Générale de la Coopération au Développement et à l'Aide humanitaire de la Belgique (DGD) and Science Policy Office of Belgium (BELSPO). A research mission of E.K.Y. in Yangambi was financed by the*Fonds Léopold III pour l'Exploration et la Conservation de la Naturein 2019. The mission of E.K.Y. in Yangambi for a complementary digitization was supported by the Ghent University-Global Minds Fund (GMF) VLIR-UOS (2020–2021). W.H. was funded by BELSPO through the AFRIFORD project (BR/132/A1; Genetic and paleoecological signatures of African rainforest dynamics: Pre-adapted to change?) and the FED-tWIN2019-prf-075 profile CongoFORCE (Congo Basin forests in a changing environment).*

Data availability Daily, monthly, and yearly precipitation and temperature data and derived indices for the period 1960–2020 in Yangambi are available on figshare: https://figshare.com/s/f8b550a145696dc10f6f.

Declarations

Competing interests The authors declare no competing interests.

Open Access This article is licensed under a Creative Commons Attribution 4.0 International License, which permits use, sharing, adaptation, distribution and reproduction in any medium or format, as long as you give appropriate credit to the original author(s) and the source, provide a link to the Creative Commons licence, and indicate if changes were made. The images or other third party material in this article are included in the article's Creative Commons licence, unless indicated otherwise in a credit line to the material. If material is not included in the article's Creative Commons licence and your intended use is not permitted by statutory regulation or exceeds the permitted use, you will need to obtain permission directly from the copyright holder. To view a copy of this licence, visit http://creativecommons.org/licenses/by/4.0/.

References

Aguilar E, Aziz Barry A, Brunet M, et al (2009) Changes in temperature and precipitation extremes in western central Africa, Guinea Conakry, and Zimbabwe, 1955–2006. J Geophys Res Atmos 114. https://doi.org/10.1029/2008JD011010

Aguirre-Gutiérrez J, Malhi Y, Lewis SL et al (2020) Long-term droughts may drive drier tropical forests towards increased functional, taxonomic and phylogenetic homogeneity. Nat Commun 11:1–10. https://doi.org/10.1038/s41467-020-16973-4

Aragão LEOC, Poulter B, Barlow JB et al (2014) Environmental change and the carbon balance of Amazonian forests. Biol Rev 89:913–931. https://doi.org/10.1111/brv.12088

Asefi-Najafabady S, Saatchi S (2013) Response of African humid tropical forests to recent rainfall anomalies. Philos Trans R Soc Lond B Biol Sci 368:20120306. https://doi.org/10.1098/rstb.2012.0306

Awange JL, Ferreira VG, Forootan E et al (2016) Uncertainties in remotely sensed precipitation data over Africa. Int J Climatol 36:303–323. https://doi.org/10.1002/joc.4346

Bates D, Mächler M, Bolker B, Walker S (2015) Fitting linear mixed-effects models using lme4. J Stat Softw 67:1–48. https://doi.org/10.18637/jss.v067.i01

Batsi G, Sonwa DJ, Mangaza L, et al (2020) Biodiversity of the Cocoa Agroforests of the Bengamisa-Yangambi Forest Landscape in the Democratic Republic of the Congo (DRC). Forests 11. https://doi.org/10.3390/f11101096

Bennett AC, Dargie GC, Cuni-sanchez A, et al (2021) Resistance of African tropical forests to an extreme climate anomaly. Proc Natl Acad Sci USA in press:

Bola GB, Tshimanga RM, Neal J et al (2022) Understanding flood seasonality and flood regime shift in the Congo River Basin. Hydrol Sci J 67:1496–1515. https://doi.org/10.1080/02626667.2022.2083966

Bush ER, Jeffery K, Bunnefeld N et al (2020) Rare ground data confirm significant warming and drying in western equatorial Africa. PeerJ 2020:1–29. https://doi.org/10.7717/peerj.8732

Chaney NW, Sheffield J, Villarini G, Wood EF (2014) Development of a high-resolution gridded daily meteorological dataset over sub-Saharan Africa: spatial analysis of trends in climate extremes. J Clim 27:5815–5835. https://doi.org/10.1175/JCLI-D-13-00423.1

Cleveland WS (1979) Robust locally weighted regression and smoothing scatterplots. J Am Stat Assoc 74:829–836. https://doi.org/10.1080/01621459.1979.10481038

Davies RB (2002) Hypothesis testing when a nuisance parameter is present only under the alternative: linear model case. Biometrika 89:484–489. https://doi.org/10.1093/biomet/89.2.484

Denbow J (2013) The Archaeology and Ethnography of Central Africa. Cambridge University Press, Cambridge

Dezfuli A, Dezfuli A (2017) Climate of Western and Central Equatorial Africa

Diem JE, Ryan SJ, Hartter J, Palace MW (2014) Satellite-based rainfall data reveal a recent drying trend in central equatorial Africa. Clim Change 126:263–272. https://doi.org/10.1007/s10584-014-1217-x

Dosio A, Jones RG, Jack C et al (2019) What can we know about future precipitation in Africa? Robustness, significance and added value of projections from a large ensemble of regional climate models. Clim Dyn 53:5833–5858. https://doi.org/10.1007/s00382-019-04900-3

Edwards DC, Mckee TB (1997) Characteristics of 20th century drought in the United States at multiple time scales. Fort Collins, Colorado

Esquivel-Muelbert A, Baker TR, Dexter KG et al (2019) Compositional response of Amazon forests to climate change. Glob Chang Biol 25:39–56. https://doi.org/10.1111/gcb.14413

Fang Y, Sun G, Caldwell P et al (2016) Monthly land cover-specific evapotranspiration models derived from global eddy flux measurements and remote sensing data. Ecohydrology 9:248–266. https://doi.org/10.1002/eco.1629

Fauset S, Baker TR, Lewis SL et al (2012) Drought-induced shifts in the floristic and functional composition of tropical forests in Ghana. Ecol Lett 15:1120–1129. https://doi.org/10.1111/j.1461-0248.2012.01834.x

Fotso-Nguemo TC, Vondou DA, Tchawoua C, Haensler A (2017) Assessment of simulated rainfall and temperature from the regional climate model REMO and future changes over Central Africa. Clim Dyn 48:3685–3705. https://doi.org/10.1007/s00382-016-3294-1

Fotso-Nguemo TC, Chamani R, Yepdo ZD et al (2018) Projected trends of extreme rainfall events from CMIP5 models over Central Africa. Atmos Sci Lett 19:0–8. https://doi.org/10.1002/asl.803

Harris I, Osborn TJ, Jones P, Lister D (2020) Version 4 of the CRU TS monthly high-resolution gridded multivariate climate dataset. Sci Data 7:1–18. https://doi.org/10.1038/s41597-020-0453-3

Hasan MM, Dunn PK (2010) A simple Poisson–gamma model for modelling rainfall occurrence and amount simultaneously. Agric for Meteorol 150:1319–1330. https://doi.org/10.1016/j.agrformet.2010.06.002

Hubau W, Lewis SL, Phillips OL et al (2020) Asynchronous carbon sink saturation in African and Amazonian tropical forests. Nature 579:80–87. https://doi.org/10.1038/s41586-020-2035-0

Huffman GJ, Adler RF, Bolvin DT et al (2007) The TRMM multisatellite precipitation analysis (TMPA): quasi-global, multiyear, combined-sensor precipitation estimates at fine scales. J Hydrometeorol 8:38–55. https://doi.org/10.1175/JHM560.1

Igri PM, Tanessong RS, Vondou DA, et al (2022) Evaluation of the Tropical Rainfall Measuring Mission (TRMM) 3B42 and 3B43 products relative to synoptic weather station observations over Cameroon. Congo Basin Hydrol. Clim. Biogeochem. 97–119

James R, Washington R, Rowell DP (2013) Implications of global warming for the climate of African rainforests. Philos Trans R Soc B Biol Sci 368. https://doi.org/10.1098/rstb.2012.0298

Jiang Y, Zhou L, Tucker CJ et al (2019) Widespread increase of boreal summer dry season length over the Congo rainforest. Nat Clim Chang 9:617–622. https://doi.org/10.1038/s41558-019-0512-y

Karam S, Seidou O, Nagabhatla N et al (2022) Assessing the impacts of climate change on climatic extremes in the Congo River Basin. Clim Change 170:40. https://doi.org/10.1007/s10584-022-03326-x

Kendall MG (1975) Rank correlation methods, 4th edn. Griffin, London

Kendon EJ, Stratton RA, Tucker S, et al (2019) Enhanced future changes in wet and dry extremes over Africa at convection-permitting scale. Nat Commun 10. https://doi.org/10.1038/s41467-019-09776-9

Kidd C, Becker A, Huffman GJ et al (2017) So, how much of the Earth's surface is covered by rain gauges? Bull Am Meteorol Soc 98:69–78. https://doi.org/10.1175/BAMS-D-14-00283.1

Laraque A, Bellanger M, Adele G et al (2013) Evolutions récentes des débits du Congo, de l'Oubangui et de la Sangha. Geo Eco Trop 37:93–100

Laraque A, Moukandi G, Orange D et al (2020) Recent budget of hydroclimatology and hydrosedimentology of the Congo River in Central Africa. Water 12(9):2613. https://doi.org/10.3390/w12092613

Laux P, Jäckel G, Munang R, Kunstmann H (2010) Impact of climate change on agricultural productivity under rainfed conditions in Cameroon—A method to improve attainable crop yields by planting date adaptations. Agric for Meteorol 150:1258–1271. https://doi.org/10.1016/j.agrformet.2010.05.008

Lu J, Sun G, McNulty SG, Amatya DM (2005) A comparison of six potential evapotranspiration methods for regional use in the Southeastern United States. J Am Water Resour Assoc 41:621–633

Luambua NK, Hubau W, Salako KV et al (2021) Spatial patterns of light-demanding tree species in the Yangambi rainforest (Democratic Republic of Congo). Ecol Evol 11:18691–18707. https://doi.org/10.1002/ece3.8443

Mabrouk EH, Moursy FI, Morsy M (2022) Assessment of climate characteristics and long-term trends of rainfall and drought in the Congo River Basin. J Water Clim Chang 13:3906–3933. https://doi.org/10.2166/wcc.2022.241

Mahé G (1995) Modulation annuelle et fluctuations interannuelles des précipitations sur le bassin versant du {C}ongo. In: Grands bassins fluviaux périatlantiques : Congo, Niger, Amazone. ORSTOM, {P}aris, pp 13–26

Malhi Y, Wright J (2004) Late twentieth-century patterns and trends in the climate of tropical forest regions. Trop for Glob Atmos Chang 359:311–329. https://doi.org/10.1093/acprof:oso/9780198567066.003.0001

Mangaza L, Sonwa D, Batsi G, et al (2021) Building a framework towards climate-smart agriculture in the Yangambi landscape, Democratic Republic of Congo (DRC). Int J Clim Chang Strateg Manag 13. https://doi.org/10.1108/IJCCSM-08-2020-0084

Mayaux P, Massart M, Cutsem C Van, et al (2003) A land cover map of Africa. European Commission, Joint Research Centerc 56p.

McCollum JR, Gruber A, Ba MB (2000) Discrepancy between gauges and satellite estimates of rainfall in equatorial Africa. J Appl Meteorol 39:666–679. https://doi.org/10.1175/1520-0450-39.5.666
Mckee TB, Doesken NJ, Kleist J (1993) The relationship of drought frequency and duration to time scales. In: Proceedings of the ninth conference on applied climatology. Am Metereological Soc 179–184
Meza F, Silva D (2009) Dynamic adaptation of maize and wheat production to climate change. Clim Change 94:143–156. https://doi.org/10.1007/s10584-009-9544-z
Muggeo V (2008) Segmented: an R package to fit regression models with broken-line relationships. R News 8:20–25
Ndehedehe CE, Agutu NO (2022) Historical changes in rainfall patterns over the Congo Basin and impacts on runoff (1903–2010). Congo Basin Hydrol. Clim. Biogeochem. 145–163
Nicholson SE, Funk C, Fink AH (2018) Rainfall over the African continent from the 19th through the 21st century. Glob Planet Change 165:114–127. https://doi.org/10.1016/j.gloplacha.2017.12.014
Nicholson SE, Klotter D, Dezfuli AK, Zhou L (2018) New rainfall datasets for the Congo basin and surrounding regions. J Hydrometeorol 19:1379–1396. https://doi.org/10.1175/JHM-D-18-0015.1
Nicholson SE, Klotter D, Zhou L, Hua W (2019) Validation of satellite precipitation estimates over the Congo Basin. J Hydrometeorol 20:631–656. https://doi.org/10.1175/JHM-D-18-0118.1
Nicholson SE (2022) The rainfall and convective regime over Equatorial Africa, with emphasis on the Congo Basin. Congo Basin Hydrol. Clim. Biogeochem. 25–48
Peterson TC, Zhang X, Brunet-India M, Vázquez-Aguirre JL (2008) Changes in North American extremes derived from daily weather data. J Geophys Res Atmos 113:1–9. https://doi.org/10.1029/2007JD009453
R Core Team (2017) R: a language and environment for statistical computing.
Raghavendra A, Zhou L, Jiang Y, Hua W (2018) Increasing extent and intensity of thunderstorms observed over the Congo Basin from 1982 to 2016. Atmos Res 213:17–26. https://doi.org/10.1016/j.atmosres.2018.05.028
Salerno J, Diem JE, Konecky BL, Hartter J (2019) Recent intensification of the seasonal rainfall cycle in equatorial Africa revealed by farmer perceptions, satellite-based estimates, and ground-based station measurements. Clim Change 153:123–139. https://doi.org/10.1007/s10584-019-02370-4
Schneider U, Becker A, Finger P et al (2014) GPCC's new land surface precipitation climatology based on quality-controlled in situ data and its role in quantifying the global water cycle. Theor Appl Climatol 115:15–40. https://doi.org/10.1007/s00704-013-0860-x
Soula S, Kasereka JK, Georgis JF, Barthe C (2016) Lightning climatology in the Congo Basin. Atmos Res 178–179:304–319. https://doi.org/10.1016/j.atmosres.2016.04.006
Sun G, Alstad K, Chen J et al (2011) A general predictive model for estimating monthly ecosystem evapotranspiration. Ecohydrology 4:245–255. https://doi.org/10.1002/eco.194
Sun Q, Miao C, Duan Q et al (2018) A review of global precipitation data sets: data sources, estimation, and intercomparisons. Rev Geophys 56:79–107. https://doi.org/10.1002/2017RG000574
Sun G (2013) How to estimate the actual evapotranspiration for tropical forests?
Tadese M, Kumar L, Koech R (2020) Long-term variability in potential evapotranspiration, water availability and drought under climate change scenarios in the Awash River Basin, Ethiopia. Atmosphere (Basel) 11. https://doi.org/10.3390/ATMOS11090883
Tsalefac M, Hiol FH, Mahe G, et al (2015) Climate of Central Africa: past, present and future. In: Wasseige C. de, Tadoum M, Eba'a Atyi R, Doumenge C (eds) The forests of the Congo Basin - forests and climate change. Weyrich, 82, Leerstoelgroep Aardsysteemkunde, 37–52
Tschora H, Cherubini F (2020) Co-benefits and trade-offs of agroforestry for climate change mitigation and other sustainability goals in West Africa. Glob Ecol Conserv 22:00919. https://doi.org/10.1016/j.gecco.2020.e00919
Verchot LV, Van Noordwijk M, Kandji S et al (2007) Climate change: linking adaptation and mitigation through agroforestry. Mitig Adapt Strateg Glob Chang 12:901–918. https://doi.org/10.1007/s11027-007-9105-6
Vicente-Serrano SM, Beguería S, López-Moreno JI (2010) A multi-scalar drought index sensitive to global warming: the standardized precipitation evapotranspiration index – SPEI. J Clim 23:1696–1718. https://doi.org/10.1175/2009JCLI2909.1
Walsh RPD, Lawler DM (1981) Rainfall seasonality: description, spatial patterns and change through time. Weather 36:201–208. https://doi.org/10.1002/j.1477-8696.1981.tb05400.x
Warton DI, Duursma RA, Falster DS, Taskinen S (2012) smatr 3– an R package for estimation and inference about allometric lines. Methods Ecol Evol 3:257–259. https://doi.org/10.1111/j.2041-210X.2011.00153.x
Washington R, James R, Pearce H, et al (2013) Congo basin rainfall climatology: can we believe the climate models? Philos Trans R Soc B Biol Sci 368. https://doi.org/10.1098/rstb.2012.0296

Wood S (2001) Minimizing model fitting objectives that contain spurious local minima by bootstrap restarting. Biometrics 57:240–244. https://doi.org/10.1111/j.0006-341X.2001.00240.x
Zhang Y (2013) Likelihood-based and Bayesian methods for Tweedie compound Poisson linear mixed models. Stat Comput 23:743–757. https://doi.org/10.1007/s11222-012-9343-7
Zhou L, Tian Y, Myneni RB et al (2014) Widespread decline of Congo rainforest greenness in the past decade. Nature 508:86–90. https://doi.org/10.1038/nature13265

Publisher's Note Springer Nature remains neutral with regard to jurisdictional claims in published maps and institutional affiliations.

Authors and Affiliations

Emmanuel Kasongo Yakusu[1,2,3] · Joris Van Acker[1] · Hans Van de Vyver[4] · Nils Bourland[2,5,6] · José Mbifo Ndiapo[7] · Théophile Besango Likwela[7] · Michel Lokonda Wa Kipifo[7] · Amand Mbuya Kankolongo[8] · Jan Van den Bulcke[1] · Hans Beeckman[2] · Marijn Bauters[9,10] · Pascal Boeckx[9] · Hans Verbeeck[10] · Kim Jacobsen[2,10] · Gaston Demarée[4] · Françoise Gellens-Meulenberghs[4] · Wannes Hubau[1,2]

✉ Emmanuel Kasongo Yakusu
emmakasongo1@yahoo.fr

1 Laboratory of Wood Technology, Department of Environment, Faculty of Bioscience Engineering, UGent-Woodlab, Ghent University, Coupure Links 653, 9000 Ghent, Belgium

2 Service of Wood Biology, Royal Museum for Central Africa, Leuvensesteenweg 13, 3080 Tervuren, Belgium

3 Faculté de Gestion des Ressources Naturelles Renouvelables, Université de Kisangani, B.P.: 2012, Avenue Kitima, 3, Kisangani, Democratic Republic of the Congo

4 Meteorological and Climatological Research, Royal Meteorological Institute of Belgium, Avenue Circulaire, 3 B-1180 Brussels, Belgium

5 Center for International Forestry Research, Situ Gede, Bogor Barat, Bogor 16115, Indonesia

6 Resources and Synergies Development, Noliktavu Iela 7, Dreilini, Stopinu Novads, Riga 2130, Latvia

7 Centre de Recherche de Yangambi, Institut National Pour La Recherche Et L'Etude Agronomiques, Yangambi, Democratic Republic of the Congo

8 Direction Générale, Institut National Pour La Recherche Et L'Etude Agronomiques, Kinshasa13, Avenue de Cliniques, Gombe, Democratic Republic of the Congo

9 Department of Green Chemistry and Technology, Isotope Bioscience Laboratory—ISOFYS, Ghent University, Coupure Links 653, 9000 Ghent, Belgium

10 Computational & Applied Vegetation Ecology, UGent-CAVElab, Ghent University, Coupure Links 653, 9000 Ghent, Belgium